Available online at www.sciencedirect.com
ScienceDirect
Gene 414 (2008) 19–31
GENE
www.elsevier.com/locate/gene

Entamoeba histolytica EhDEAD1 is a conserved DEAD-box RNA helicase with ATPase and ATP-dependent RNA unwinding activities

César López-Camarillo [a], María de la Luz García-Hernández [b,1], Laurence A. Marchat [c], Juan P. Luna-Arias [d], Olga Hernández de la Cruz [a], Leobardo Mendoza [a], Esther Orozco [b,*]

[a] *Universidad Autónoma de la Ciudad de México, Posgrado en Ciencias Genómicas, México DF, México*
[b] *CINVESTAV-IPN, Departamento de Patología Experimental, México DF, México*
[c] *ENMH-IPN, Programa Institucional de Biomedicina Molecular, México DF, México*
[d] *CINVESTAV-IPN, Departamento de Biología Celular, México DF, México*

Received 21 April 2007; received in revised form 21 December 2007; accepted 30 January 2008
Available online 16 February 2008

Abstract

RNA helicases are widely conserved key enzymes that perform multiple functions in RNA metabolism. Here, we present the cloning, expression and functional characterization of the EhDEAD1 RNA helicase in the protozoan parasite *Entamoeba histolytica*. According to its primary structure, EhDEAD1 is evolutionary related to yeast DED1 and human DDX3X RNA helicases, both involved in translation and cell cycle regulation. The EhDEAD1 predicted amino acid sequence exhibits the nine conserved motifs described for the DEAD-box SFII superfamily members reported in other organisms and it is evolutionary close to protozoan homologues. Purified recombinant EhDEAD1 protein presented ATPase activity and it was able to bind and unwind RNA in an ATPase-dependent manner *in vitro*. RT-PCR assays showed that *EhDead1* gene is overtranscribed in the cell cycle S phase. Moreover, inhibition of *EhDead1* gene expression by antisense RNA seemed to facilitate transition from S to G2/M phase. Intriguingly, our results showed that EhDEAD1 was unable to rescue two yeast *Ded1* RNA helicase mutants affected in translation, in spite of the high sequence homology with yeast DED1.

Keywords: Protozoan parasite; Amoebiasis; Posttranscriptional regulation; RNA metabolism

1. Introduction

In eukaryotes, RNA helicases catalyze RNA unwinding and secondary structures rearrangements that are required steps for transcription, ribosome biogenesis, pre-mRNA processing, mRNA export, degradation, interference and translation (Linder and Daugeron, 2000; Tanner and Linder, 2001; Linder, 2006; Fuller-Pace, 2006). In addition, RNA helicases regulate cell cycle events and differentiation processes and participate as RNPases that remodel RNA–protein interactions (Schwer, 2001). The DEAD/DExH-box SFII RNA helicase superfamily is characterized by the presence of the well conserved DEAD (Asp-Glu-Ala-Asp) or DExH (Asp-Glu-x-His) motif II that together with other functional elements (eight and seven in DEAD and DExH-box proteins, respectively) form the helicase domain required for RNA binding and ATP-dependent unwinding activities (Gorbalenya and Koonin, 1993; Tanner et al., 2003; Rocak and Linder, 2004; Linder, 2006). Yeast DED1 is a DEAD-box RNA helicase that is essential for translation and cell cycle regulation (Chuang et al., 1997), whereas its human orthologues, DDX3X and DDX3Y proteins, participate in mRNA export and cell cycle regulation,

Abbreviations: aa, amino acid; BLAST, basic local alignment search tool; bp, base pair; CE, cytoplasmic extract; IPTG, isopropyl-beta-D-thiogalactopyranoside; MESG, 2-amino-6-mercapto-7-methylpurine riboside; NE, nuclear extract; nt, nucleotide; PNP, purine nucleoside phosphorylase.

* Corresponding author. CINVESTAV-IPN, Departamento de Patología Experimental, Av. IPN # 2508, Col. San Pedro Zacatenco, CP 07360, México DF, México. Tel.: +52 55 5061 3800x5650; fax: +52 55 5061 3800x5672.
E-mail address: esther@cinvestav.mx (E. Orozco).
[1] Present address: Norris Comprehensive Cancer Center, USC, Department of Molecular Microbiology and Immunology, Los Angeles CA, USA.

0378-1119/$ - see front matter © 2008 Elsevier B.V. All rights reserved.
doi:10.1016/j.gene.2008.01.024

respectively (Yedavalli et al., 2004; Sekiguchi et al., 2004). The *Xenopus laevis* AN3 protein, another yeast DED1 orthologue, is a mRNA export factor (Gururajan et al., 1991). Recently, computational analyses led to the identification of large RNA helicases families in the protozoan parasites *Leishmania major* (Ivens et al., 2005) and *Plasmodium falciparum* (Tuteja and Pradhan, 2006), but most proteins remain uncharacterized.

Entamoeba histolytica is the protozoan responsible for human amoebiasis that affects 500 million people around the world (Jackson, 2000). Our interest in elucidating gene expression regulation and understanding the molecular mechanisms involved in transcription and mRNA processing (Marchat et al., 2002; Mendoza et al., 2003; de Dios-Bravo et al., 2005; Lopez-Camarillo et al., 2003; Lopez-Camarillo et al., 2005; Garcia-Vivas et al., 2005) led us to study RNA helicases in this parasite. Taking advantage of the recent completion of the *E. histolytica* genome sequence (Loftus et al., 2005), we have extensively screened databases and found 33 potential genes encoding proteins with significant similarity to DEAD and DExH-box RNA helicases (Marchat et al., submitted for publication). In this paper, we have focused on the characterization of EhDEAD1 (GenBank Accession number: XP_653330), the *E. histolytica* homologue of human DDX3X and yeast DED1 proteins. Our results evidenced that EhDEAD1 is a DEAD-box RNA helicase with ATPase, RNA binding and RNA unwinding activities *in vitro*, that seems to be important for cell cycle regulation.

2. Materials and methods

2.1. In silico analysis of EhDEAD1 protein sequence

The predicted amino acid (aa) sequence of EhDEAD1 was used to determine identity/homology percentages and *e* values to related proteins by BLAST (http://www.expasy.org/tools/blast/). Homologous protein sequences from diverse organisms were aligned by ClustalW software (http://www.ch.embnet.org/software/ClustalW.html/), allowing gap penalties of 10 to maximize protein homology. Structural domains and sequence patterns were predicted by Motif Scan (http://myhits.isb-sib.ch/cgi-bin/motif_scan) and Scan Prosite (http://www.expasy.org/tools/scanprosite/) programs. For phylogenetic studies, conserved helicase domains of EhDEAD1 and its closest homologues were aligned using ClustalW to construct the corresponding tree by the Neighbor-Joining method through the Molecular Evolutionary Genetics Analysis MEGA software version 3.1 (Kumar et al., 2004). The robustness of the phylogenetic inference was assessed by bootstrap analyses with 1000 replications of the data, based on criteria of 50% majority-rule consensus.

2.2. E. histolytica cultures

Trophozoites of clones A (strain HM1:IMSS) were axenically cultured in TYI-S-33 medium (15% serum) (Diamond et al., 1978) and used in logarithmic growth phase for all experiments. Serum starvation was carried out by incubating growing trophozoites of clone A in TYI-S-33 medium with 2% serum for 16 h at 37 °C (Vohra et al., 1998). Cultures of clone L6 (strain HM1:IMSS) were synchronized using complete TYI-S-33 medium with 200 μg/ml colchicine for 24 h. Then, cells were transferred to fresh medium and harvested at 0, 3, 8 and 12 h to obtain trophozoites in M, G1, S and G2 phase, respectively (Orozco et al., 1988). To confirm cell cycle synchronization, we used medium supplemented with 5 μCi/ml [^{3}H] thymidine; cell number and the amount of radioactivity incorporated in DNA (cpm) were determined at 4 h intervals as previously reported (Orozco et al., 1988). Three independent assays were performed.

2.3. Northern blot analysis

Total RNA (20 μg) was extracted from clone A trophozoites using Trizol reagent (Invitrogen), separated on agarose-formaldehyde gel and transferred to a nylon membrane. The specific *EhDead1* probe (663–705 nucleotide (nt)) was randomly labeled with [α-^{32}P]dATP by the Prime gene kit (Promega). Then, blots were incubated overnight with specific *EhDead1* probe, stringently washed and exposed to X-ray film at −70 °C for up to 2 weeks. Molecular size of labeled mRNA was calculated by comparison with known RNA markers (0.24–9.5 kb, Invitrogen).

2.4. RT-PCR assays

cDNA was synthesized using 1 μg of total RNA from trophozoites of clone A and cell cycle synchronized trophozoites of clone L6, 100 ng of oligo (dT_{18}), 100 mM DTT, 10 mM dNTPs, 40 U of SUPERase-in (Ambion) and 200 U of Superscript II reverse transcriptase (Invitrogen) in first-strand buffer, for 1 h at 42 °C. Semi-quantitative PCR assays were performed using *EhDead1a-S* (5′-CCGGATCCATGGCTTACGTACCACCA-3′) sense, *EhDead1b-S* (5′-CCGGATCCATGCCAGTCCAAAAAGCAA-3′) sense and *EhDead1b-AS* (5′-CCAAGCTTATCAAACATATGAGGTTTT-3′) antisense primers. As an internal control, we used the *actin* (5′-AGCTGTTCTTTCATTATATGC-3′) sense and (5′-TTCTCTTTCAGCAGTAGTGGT-3′) antisense specific primers. RT-PCR products were separated through 1% agarose gel electrophoresis, ethidium bromide stained and observed in a Gel-Doc apparatus (Bio-Rad). For densitometric analysis, we used the Quantity One software (Bio-Rad). Three independent assays were performed.

2.5. Cloning and sequencing of EhDead1 gene

The first 447 bp and the last 1272 bp (463–1734 nt) of the *EhDead1* full-length sequence (1734 nt) (Accession no.: XM_648238) reported at locus EHI-175030 in the *E. histolytica* Pathema database (http://pathema.tigr.org/tigr-scripts/Entamoeba/PathemaHomePage.cgi) were PCR amplified from genomic DNA of trophozoites of clone A using *EhDead1a-S* sense and *EhDead1a-AS* (5′-CCAAGCTTCATAACATTTTTAAAGC-3′) antisense specific primers, and *EhDead1b-S* sense and *EhDead1b-AS* antisense specific primers, respectively. PCR products were cloned in frame into BamHI and HindIII restriction sites of pRSET A vector to generate the recombinant pRSET-$EhDead1_{17}$ and pRSET-$EhDead1_{48}$ plasmids, respectively. Both constructs were confirmed by automated DNA sequencing.

2.6. Expression and purification of recombinant $EhDEAD1_{17}$ and $EhDEAD1_{48}$ polypeptides

Escherichia coli BL21(DE3)pLysS were transformed with the plasmids described above and treated with 1 mM isopropyl-beta-D-thiogalactopyranoside (IPTG) for 3 h. The recombinant polypeptides, $rEhDEAD1_{17}$ (1–149 aa corresponding to the amino terminus) and $rEhDEAD1_{48}$ (155–578 aa including the helicase domain), were expressed as 6x-His-tagged fusion proteins and purified under native or denaturing conditions through Ni^{2+}-NTA agarose affinity chromatography (Qiagen). The identity of $rEhDEAD1_{17}$ and $rEhDEAD1_{48}$ polypeptides was confirmed by Western blot assays using anti-6x-His-tag monoclonal antibodies (Roche) and the ECL-Plus detection system (Amersham).

2.7. Production of anti-EhDEAD1 antibodies and Western blot assays

Five Balb-c mice and a New Zealand rabbit were inoculated with 150 μg of purified $rEhDEAD1_{17}$ or $rEhDEAD1_{48}$ polypeptides, respectively, in complete Freund's adjuvant at days 0 and seven. At day 60, animals received 100 μg of each polypeptide in incomplete Freund's adjuvant. Seven days after the last inoculation, immune sera were collected and stored at −20 °C. For Western blot assays, nuclear (NE) and cytoplasmic (CE) extracts were obtained from trophozoites of clone A, separated on 10% SDS-PAGE (20 μg/lane) and electrotransferred to nitrocellulose membranes. Membranes were incubated with immune sera (1/1000) in 5% nonfat dry milk and 0.05% Tween-20 in PBS pH 7.4 overnight at 4 °C. Proteins were detected by peroxydase-conjugated secondary antibodies (1/1500) (Zymed) and the ECL-Plus system (Amersham). As controls, we used anti-EhPC4 antibodies that specifically identified the *E. histolytica* putative transcription and polyadenylation factor PC4 in the nuclear fraction (our unpublished data) and antibodies against the Poly(A) polymerase (EhPAP) protein that has been previously located in both CE and NE (Garcia-Vivas et al., 2005).

2.8. Laser confocal microscopy assays

For immunofluorescence assays, trophozoites of clone A were cultured on cover slides, fixed with 4% paraformaldehyde for 40 min at 37 °C and permeabilized with acetone. Cells were blocked with 2% BSA in PBS for 60 min at 37 °C, washed four times with 0.2% Triton-X100/PBS and incubated with rabbit anti-$rEhDEAD1_{48}$ antibodies (1:200) overnight at 4 °C. Cells were washed again four times and incubated with fluorescein-labeled secondary antibodies (1:200) for 1 h at 37 °C. Finally, DNA was counterstained for 10 min with 4′,6-diamidino-2-phenylindole, dihydrochloride (DAPI) (5 μg/ml). Samples were analyzed through an inverted microscope (DIM IRE2, Leica Microsystem) attached to a laser confocal scanning system Leica TCS SP2 (Leica, CO).

2.9. RNA electrophoretic mobility shift assays (REMSA)

REMSA were performed using a 256 nt RNA probe corresponding to the $PSIII^{156}$ fragment that contains the last 100 nt of the open reading frame and 156 nt of the 3′UTR of the *EhPgp5* gene (Lopez-Camarillo et al., 2003). The RNA probe was [α-^{32}P]UTP labeled by *in vitro* transcription using T7 RNA polymerase (Promega). Purified $rEhDEAD1_{48}$ (5–15 nM) and RNA probe (5×10^5 cpm) were incubated in binding buffer for 15 min at 4 °C and RNA–protein complexes were resolved through 6% non-denaturing PAGE (Lopez-Camarillo et al., 2003). Gels were vacuum-dried, and radioactive complexes were detected in a Phosphor Imager apparatus (Bio-Rad). Three independent assays were performed.

2.10. ATPase activity assays

ATPase activity of $rEhDEAD1_{48}$ was measured *in vitro* using the EnzChek Phosphate Assay Kit (Molecular Probes) as described by the manufacturer. Briefly, reaction mixtures containing 50 μl of 20× reaction buffer, 400 μM ATP, 1 mM KCl, 1 mM NaCl, 200 μl of the substrate 2-amino-6-mercapto-7-methylpurine riboside (MESG), 10 μl of purine nucleoside phosphorylase (PNP, 1U), and 5 μg of *E. histolytica* total or poly(A^+) RNA in a final volume reaction of 1 ml, were pre-incubated for 10 min at 22 °C. $rEhDEAD1_{48}$ (5 nM) was added and absorbance at 360 nm (A_{360}) was measured at different times through a Beckman spectrophotometer. The inorganic phosphate (Pi) released from ATP by $rEhDEAD1_{48}$ is consumed by the enzymatic MESG/PNP reaction that is detected by an increase in A_{360}, which is therefore a representation of $rEhDEAD1_{48}$ATPase activity (Webb, 1992). Yeast total RNA was used as a control. Three independent assays were performed in duplicate.

2.11. RNA unwinding assays

RNA templates for unwinding reactions were synthesized from two linear double stranded DNA fragments containing the T7 promoter sequence at both ends. Two fragments of 246 and 216 nt were amplified from a plasmid containing the 3′ UTR of the *EhPgp5* gene, using the 3′UTR-Pgp5-S (5′-GTAGGAGGTGCAGTATTTCC-3′) sense, and T7-3′UTR-Pgp5-127AS (5′-GCGTAATACGACTCACTATAGGGTTTAAGTCATTAACATA A-3′) antisense primers, and T7-3′UTR-Pgp5-54S (5′-GCGTAATACGAC TCACTATAGGG ATTATACACTTGCTATGC-3′) sense and 3′UTR-Pgp5-280AS (5′-AAACTGA TTATATAATTAT-3′) antisense primers, respectively (T7 promoter sequence in primers is underlined). Then, two transcripts, one in sense and another in antisense orientation, were synthesized by *in vitro* transcription from DNA templates using the T7 RNA polymerase. Single stranded RNA (ssRNA) probes were annealed by heating at 95 °C for 7 min, followed by slow cooling down to 4 °C. RNA unwinding reactions were carried out in 20 ml reaction volume containing 10 mM HEPES (pH 8.0), 40 mM KCl, 4 mM $MgCl_2$, 1 mM DTT, 5% glycerol, 20 U of RNase inhibitor, and 500 ng of RNA duplexes. Reactions were initiated by adding $rEhDEAD1_{48}$ (2–16 nM) in the presence or absence of 20 mM ATP. Samples were incubated for 30 min at 37 °C and resolved through non-denaturing 12% PAGE. Gels were ethidium bromide stained and analyzed in a Gel-Doc apparatus (Bio-Rad).

2.12. Inhibition of EhDead1 gene expression by antisense RNA

The p*NeoEhDead1-AS* plasmid containing the *EhDead1* gene cloned in antisense orientation, was constructed by replacing the choramphenicol acetyl transferase gene (*CAT*) into the p*Neo-CAT* plasmid (Hamann et al., 1995). Transfections with p*NeoEhDead1-AS* and p*Neo-CAT* control plasmids were done by electroporation of 1×10^7 trophozoites of clone A as described (Hamann et al., 1995). Drug selection was started 48 h after transfection using medium supplemented with 40 μg/ml G418 and growth of transfected trophozoites was assessed by cell counting. Then, trophozoites were submitted to serum deprivation (Section 2.2) and analyzed by flow scanning cytometry.

2.13. Analysis of DNA content by flow scanning cytometry

Transfected and non-transfected trophozoites were fixed in 70% ethanol, treated with RNase (10 mg/ml) for 1 h at room temperature (RT), and incubated with propidium iodide (PI) (0.5 mg/ml) for 1 h at RT in the dark. For DNA content measurement, flow cytometry analyses were carried out in a FACS Calibur flow cytometer (Becton Dickinson) equipped with a single laser system (6 W Innova 90-6 argon ion laser). Cells were excited with 488 nm light, and emission was measured through DF20 for PI fluorescence. Data from 5×10^6 cells were recorded for each experiment using the FACS SOFT program and analyzed by the MOTFITT software. Independent assays were done three times by duplicate.

2.14. Yeast complementation assays

S. cerevisiae isogenic strains YTC74 (*ded1::TRP1 ura3-52 lys2-801 ade2-101 trp1-Δ1 his3-Δ200 leu2-Δ1* pDED1008), YTC180 (*ded1::TRP1 ura3-52 lys2-801 ade2-101 trp1-Δ1 his3-Δ200 leu2-Δ1* pDED1021), and YTC181 (*ded1::TRP1 ura3-52 lys2-801 ade2-101 trp1-Δ1 his3-Δ200 leu2-Δ1* pDED1022) were kindly given by Dr. Jean-Leon Chong. pDED1008 plasmid contains the 2834 bp DNA fragment harboring the yeast *ded1* gene cloned into pRS316 (*URA3*) plasmid. pDED1021 is pRS315 (*LEU2*) containing the *ded1-120* mutant allele. pDED1022 is pRS315 (*LEU2*) carrying the *ded1-199* mutant allele (Chuang et al., 1997). 1PDYS (5′-CCGCTCGAGAAAAAAAATATAAAAGAGAT-3′) sense and 3PDYAS (5′-**TGCTTTTTGGACTGGCAT**AATAT-GAAATGCTTTTCTTGTT GT-3′) antisense primers were used to amplify a 127 bp DNA fragment of the yeast *ded1* gene promoter and the first 18 bp of the $EhDead1_{48}$ gene from pDED1008 plasmid. 2DEHS (5′-ACAA CAAGAAAAG-CATTTCATATT**ATGCCAGTCCAAAAAGCA**-3′) sense and 4DEHAS (5′-CACCCTAGTTTGTCTGAAA**TCAAT-CAAACATATGAGGTTTTATTGG**-3′) antisense primers were used to amplify a 1318 bp fragment of the $EhDead1_{48}$ gene from plasmid pRSET-$EhDead1_{48}$, and 5UTR3DYS (5′-**CCAATAAAACCTCATATGTTTGATTGA**TTTCAGA-CAAACTAGGGTG-3′) sense and 6UTR3DYAS (5′-GCGTGTCGACGATGATCCTTATGAT-3′) antisense primers were used to amplify a 944 bp DNA fragment spanning the yeast *ded1* 3′UTR from plasmid pDED1008 (*EhDead1* gene sequence is in bold letters). PCR amplified products were assembled and PCR amplified using primers 1PDYS and 6UTR3DYAS (Dillon and Rosen, 1990). Then, the 2301 bp full-length fragment was cloned into the XhoI and SalI restriction sites of pRS316 to generate the pRS316-*EhDead1* construction that was used to transform YTC180 or YTC181 competent yeast (Chuang et al., 1997). Transformants JP1 (YTC180 pRS316-*EhDead1*), JP2 (YTC181 pRS316-*EhDead1*), JP3 (YTC180 pDED1008) and JP4 (YTC181 pDED1008) were selected in SC-Leu-Ura-Trp. All strains were cultured in the corresponding medium at 30 °C and 15 °C.

3. Results

3.1. EhDEAD1 is a conserved DEAD-box RNA helicase of the SFII superfamily

The gene reported at locus EHI-175030 in the *E. histolytica* Pathema database (http://pathema.tigr.org/tigr-scripts/Entamoeba/PathemaHomePage.cgi) is a 1734 bp intronless gene that predicts a 66.2 kDa polypeptide. BLAST analysis of the deduced aa sequences showed the highest *e* values (*e*-104 to *e*-121) for DEAD-box RNA helicases of the DDX3X/DED1 subfamily, confirming the TIGR and Pathema annotation. The gene corresponding to the Genbank entry XM_648238 and analyzed here, was therefore called *EhDead1*. The predicted EhDEAD1 protein sequence presented 44–50% identity and 59–70% similarity to *H. sapiens* DDX3X and DDX3Y, *X. laevis* AN3, *Mus musculus* PL10 and *S. cerevisiae* DED1 RNA helicases (Table 1). The EhDEAD1 helicase domain, located from aa 145 to 490, contains the eight highly conserved motifs I (175–182 aa: AQTGSGKT), Ia (220–225 aa: PTRELG), Ib (267–272 aa: ATPGRL), II (293–296 aa: DEAD), III (328–330 aa: SAT), IV (392–394 aa: VIF), V (449–453 aa: SRGLD) and VI (472–483 aa: YVHRVGRTGRAG) of the SFII superfamily of DEAD-box proteins that are required for ATP hydrolysis, and RNA binding and

Table 1
Comparisons of EhDEAD1 protein with related DEAD-box RNA helicases

Protein name	Organism	Accession number[a]	*e*-value	H[b] (%)	I[c] (%)	Cellular functions
DDX3Y	*Hs*	O15523	*e*-121	60	44	Spermatogenesis
DDX3X	*Hs*	O00571	*e*-120	60	45	mRNA export, translation, cell cycle
AN3	*Xl*	P24346	*e*-120	64	48	mRNA export, development
PL10	*Mm*	P16381	*e*-119	59	44	mRNA translation
RH37	*At*	Q84W89	*e*-117	61	45	Unknown
DED1	*Sc*	P06634	*e*-111	70	50	mRNA translation, cell cycle
Helicase	*Tc*	Q4DC19	*e*-106	68	50	Unknown
Helicase	*Lm*	Q4Q5P5	*e*-104	65	48	Unknown

[a]UniProtknowledgebase database.
[b]Homology (H) and [c]identity (I) values are expressed in percentage (%).
Eh, *Entamoeba histolytica*; *Hs*, *Homo sapiens*; *Xl*, *Xenopus laevis*; *Mm*, *Mus musculus*; *At*, *Arabidopsis thaliana*; *Sc*, *Saccharomyces cerevisiae*; *Tc*, *Trypanosoma cruzi*; *Lm*, *Leishmania major*.

A

```
                    ---Q----                    ---I---
HsDDX3Y    MGEIIMGNIELTRYTRPTPVQKHAIPIIKGKRDLMACAQTGSGKTAAFLLPILSQIYTDG 244
ScDED1     LDGLLLENIKLARFTKPTPVQKYSVPIVANGRDLMACAQTGSGKTGGFLFPVLSESFKTG 208
EhDEAD1    LGEELDHNIFKAGFYHPMPVQKATIPIVLDKRDLMSCAQTGSGKTAAFLFPIISDILKNP 197
           :.  :  **  : : :* **** ::**: . ****:*********..**:*::*:  .

                                  -Ia--
HsDDX3Y    PGEALKAVKENGRYGRRKQYPISLVLAPTRELAVQIYEEARKFSYRSRVRPCVVYGGADI 304
ScDED1     PS---PQPESQGSFYQRKAYPTAVIMAPTRELATQIFDEAKKFTYRSWVKACVVYGGSPI 266
EhDEAD1    PM-----PRQSNFSHRVTVFPVALILAPTRELGQQIYEEAVRFTEDTPIRSVCVYGGSDS 252
           *       ....   : . :* ::::******. **::** :*:  : ::.  ****:

                        --Ib--                  -II-
HsDDX3Y    GQQIRDLERGCHLLVATPGRLVDMMERGKIGLDFCKYLVLDEADRMLDMGFEPQIRRIVE 364
ScDED1     GNQLREIERGCDLLVATPGRLNDLLERGKISLANVKYLVLDEADRMLDMGFEPQIRHIVE 325
EhDEAD1    YTQIQEMGKGCDILVATPGRLLYFTEKKIVSLSSVRYLIFDEADRMLDMGFEPQIREICE 312
             *:::: :**.:********  : *:  :.*   :**::****************.* *

                        III
HsDDX3Y    QDTMPPKGVRHTMMFSATFPKEIQMLARDFLDEYIFLAVGRVGSTSENITQKVVWVEDLD 424
ScDED1     DCDMTPVGERQTLMFSATFPADIQHLARDFLSDYIFLSVGRVGSTSENITQKVLYVENQD 385
EhDEAD1    DNEMPPVGKRQTLMFSATFPKQIQRLAADFLDDYVFITVGRAGSTVESIQQIILWVEEEI 372
           :  *.* * *:*:******* :** ** ***.:*:*::***.*** *.* * :::**:

                           IV
HsDDX3Y    KRSFLLDILGATG-SDSLTLVFVETKKGADSLEDFLYHEGYACTSIHGDRSQRDREEALH 483
ScDED1     KKSALLDLLSAS--TDGLTLIFVETKRMADQLTDFLIMQNFRATAIHGDRTQSERERALA 443
EhDEAD1    KQEAILDVLGEFAGKGQKTVIFVETKRGADILENYLYDHGYKVDSIHGDRSQADRDFSLK 432
            *:. :**:*.    ..  *::*****: ** * ::*  ..:   :*****:* :*: :*

                        --V--                   -----VI-----
HsDDX3Y    QFRSGKSPILVATAVAARGLDISNVRHVINFDLPSDIEEYVHRIGRTGRVGNLGLATS 541
ScDED1     AFRSGAATLLVATAVAARGLDIPNVTHVINYDLPSDVDDYVHRIGRTGRAGNTGLATA 501
EhDEAD1    RFKENVIQLLVATDVASRGLDIPDIEVVINYDMPNEIESYVHRVGRTGRAGKKGTAIT 490
            *:..   :**** **:*****.::  ***:*:*.:::.****:*****.*: * * :
```

B

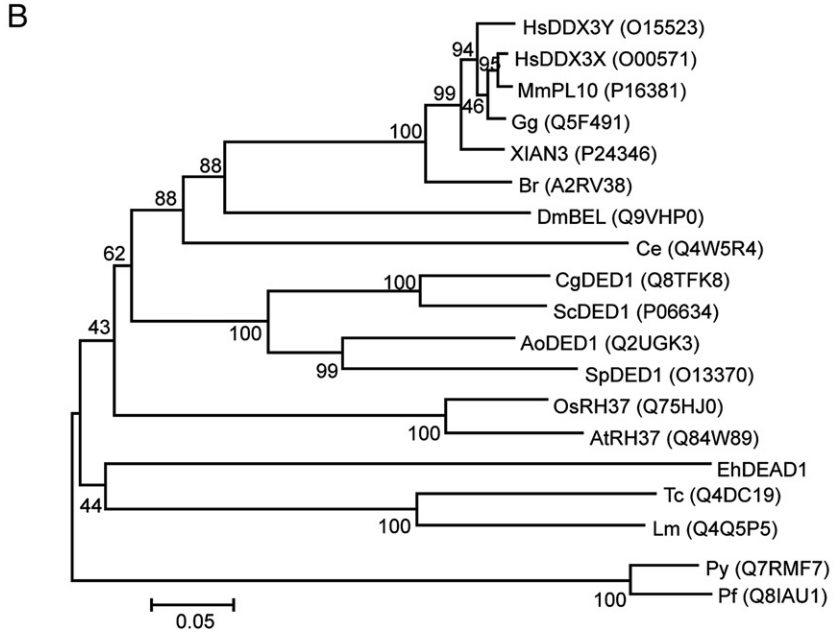

Fig. 1. Comparison of the predicted amino acids sequence of EhDEAD1, yeast DED1 and human DDX3Y RNA helicases. (A) Multiple sequence alignments were performed using ClustalW. Star, identical residues; point, conserved substitutions. Consensus RNA helicase motifs are indicated. Numbers (right) correspond to the aa position relative to the first Met in each protein. (B) Phylogenetic analysis of EhDEAD1-related RNA helicases. The rooted tree was created with the MEGA 3.1 program based on ClustalW alignments of the conserved helicase domains. Numbers on tree nodes represent the bootstrap proportions (%) of 1000 replications. *Ao*, *Aspergillus oryzae*; *At*, *Arabidopsis thaliana*; *Br*, *Brachydanio rerio*; *Ce*, *Caenorhabditis elegans*; *Cg*, *Candida glabrata*; *Dm*, *Drosophila melanogaster*; *Eh*, *Entamoeba histolytica*; *Gg*, *Gallus gallus*; *Hs*, *Homo sapiens*, *Lm*, *Leishmania major*; *Mm*, *Mus musculus*; *Os*, *Oryza sativa*; *Pf*, *Plasmodium falciparum*; *Py*, *P. yoeli*; *Sc*, *Saccharomyces cerevisiae*; *Sp*, *Schizosaccharomyces pombe*; *Tc*, *Trypanosoma cruzi*; *Xl*, *Xenopus laevis*.

unwinding activities (Gorbalenya and Koonin, 1993; Rocak and Linder, 2004). The recently described Q motif (GFYHPMPVQ), which forms a loop–helix–loop structure involved in the interaction with motif I and ATP (Tanner et al., 2003) also appeared in the predicted aa sequence, located from residue 150 to 158 (Fig. 1A). In contrast, the amino and carboxyl terminal ends of EhEAD1 present higher divergence with other homologous proteins. Phylogenetic inference indicated a clade distribution according to evolutionary scale. Protozoan parasite homologues appeared at the bottom of the tree, being EhDEAD1 close to RNA helicases from *Leishmania*, *Trypanosoma* and *Plasmodium*. EhDEAD1 is also highly related to yeast DEAD1, frog AN3 and human DDX3Y and DDX3X proteins, among others (Fig. 1B).

3.2. EhDead1 gene is transcribed as a 1.3 kb truncated transcript

To investigate whether the *EhDead1* gene was transcribed, we first performed Northern blot assays using a specific *EhDead1* gene probe, as described above. Surprisingly, we detected a single 1.3 kb band, whereas the *EhDead1* full-length transcript was expected as a 1.7 kb band (Fig. 2A, lane 1). RNA integrity was confirmed through agarose gel electrophoresis and ethidium bromide staining (Fig. 2A, lane 2). Next, we performed RT-PCR experiments using two pairs of specific primers to amplify the full-length *EhDead1* gene and the last 1272 bp of the gene (from the third ATG codon) (Fig. 2B and C). The use of the second ATG located at 49 nt position was discarded since it would generate a 1686 nt transcript. No product was obtained with the *EhDead1a-S* and *EhDead1b-AS* primers, whereas the *EhDead1b-S* and *EhDead1b-AS* primers allowed the amplification of a 1272 bp fragment. This suggested that the 5′ end of the *EhDead1* gene was not transcribed or that the *Ehdead1* mRNA was posttranscriptionally processed to generate a 5′ truncated transcript.

3.3. EhDead1 gene is expressed as a 48 kDa polypeptide that is localized in cytoplasm and nucleus

To determine the molecular weight of the EhDEAD1 protein expressed by trophozoites, we generated specific antibodies

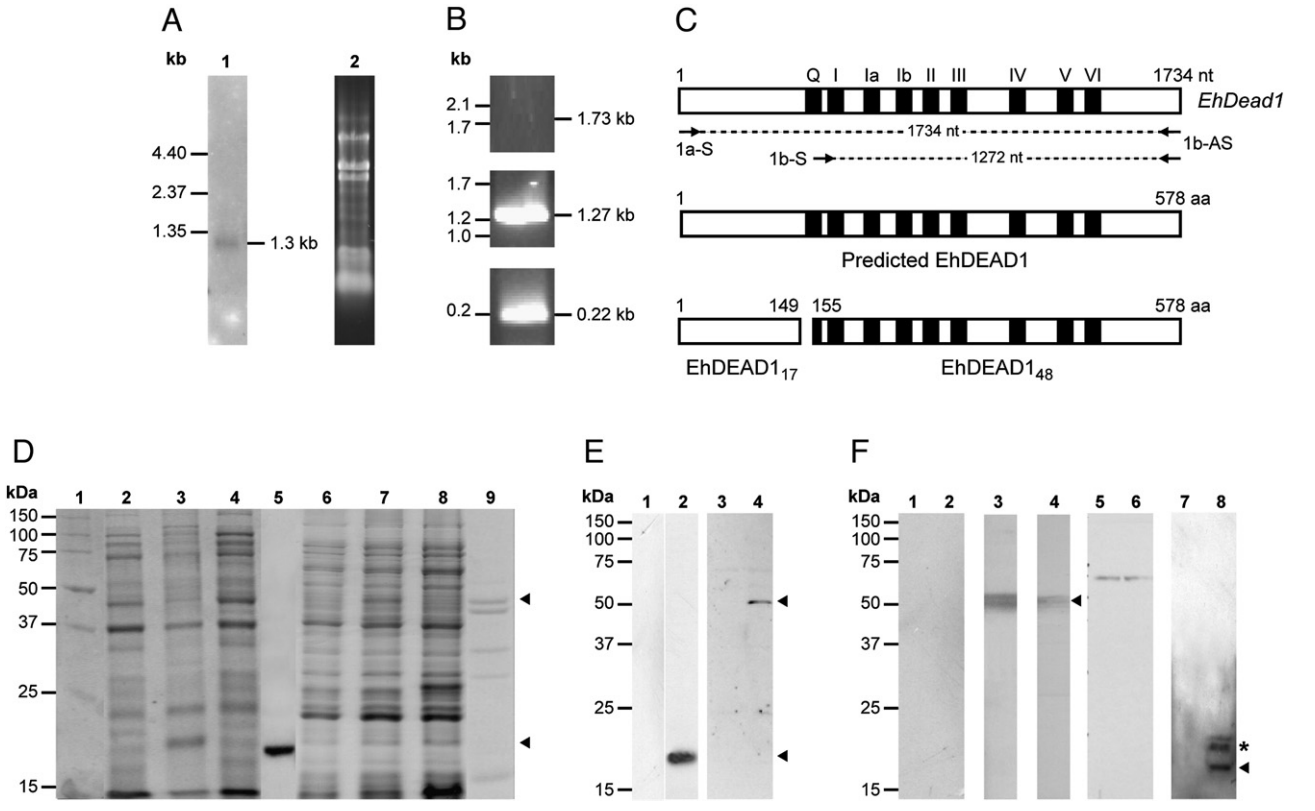

Fig. 2. Expression of the *EhDead1* gene. (A) Northern blot. Total RNA from clone A trophozoites was separated on agarose-formaldehyde gel (lane 2) transferred to a nylon membrane and hybridized with a specific *EhDead1* [α-^{32}P]-dATP labeled probe (lane 1). (B) RT-PCR assays. Full-length *EhDead1* (up), *EhDead1$_{48}$* (middle) and *actin* (bottom) genes were amplified using 1 μg of total RNA of trophozoites (clone A) and specific oligonucleotides. Products were analyzed in 1% agarose gel. (C) Schematic representation of the full-length *EhDead1* gene (up), predicted EhDEAD1 protein (middle), EhDEAD1$_{17}$ and EhDEAD1$_{48}$ polypeptides (bottom). Black box, conserved motifs of the RNA helicase domain. Arrows, oligonucleotides positions used for RT-PCR assays in B. (D) Expression and purification of rEhDEAD1$_{17}$ and rEhDEAD1$_{48}$ polypeptides. Proteins were separated through 10% SDS-PAGE and gels were stained with Coomassie blue. Lane 1, molecular weight markers; lanes 2 and 6, bacteria extracts; lanes 3 and 7, IPTG induced bacteria extract; lanes 4 and 8, IPTG induced bacteria extract after passing throughout the Ni^{2+}-NTA affinity column; lanes 5 and 9, affinity purified polypeptide. Arrowhead, recombinant polypeptides. (E) Immunodetection of purified rEhDEAD1$_{17}$ and EhDEAD1$_{48}$ by Western blot assays using anti-6x-His tag antibodies. Lanes 1 and 3, bacteria extracts; lane 2, rEhDEAD1$_{17}$; lane 4, rEhDEAD1$_{48}$. Arrowhead, recombinant polypeptides. (F) Immunodetection of native EhDEAD1 in cytoplasmic (CE) and nuclear extracts (NE) by Western blot assays using specific antibodies against rEhDEAD1$_{17}$ (lanes 1 and 2) and rEhDEAD1$_{48}$ (lanes 3 and 4). Antibodies against EhPAP (lanes 5 and 6) and EhPC4 (lanes 7 and 8) were used as controls. Lanes 1, 3, 5 and 7, CE; lanes 2, 4, 6 and 8, NE. Arrowheads, EhDEAD1 (lanes 3 and 4) and EhPC4 (lane 8). Asterisk, posttranslational modified EhPC4.

raised against the amino or the carboxyl terminal end of the full-length EhDEAD1 predicted protein. We amplified two DNA fragments: one containing the first 447 bp and another containing the last 1272 bp (including the helicase domain) of the *EhDead1* gene reported in the Pathema database. Both fragments were independently cloned into the pRSET A vector and expressed in bacteria as 6x-His-tagged recombinant rEhDEAD1$_{17}$ and rEhDEAD1$_{48}$ polypeptides, respectively. The induction and purification of both recombinant proteins were corroborated through gel electrophoresis (Fig. 2D) and Western blot assays using commercial antibodies against the 6x-His tag (Fig. 2E). The antibodies recognized a single 17 kDa protein purified from bacteria expressing rEhDEAD$_{17}$ (lane 2) and a 48 kDa band in the lane corresponding to the purified rEhDEAD1$_{48}$ polypeptide (lane 4). No signal was detected in protein extracts from non-induced bacteria (lanes 1 and 3).

Specific antibodies raised against rEhDEAD1$_{17}$ and rEhDEAD1$_{48}$ polypeptides were generated in mouse and rabbit, respectively, and used in Western blot assays to detect the native EhDEAD1 protein in nuclear (NE) and cytoplasmic (CE) extracts. In agreement with Northern blot and RT-PCR assays, mouse antibodies raised against rEhDEAD1$_{17}$ did not recognize any band in CE nor NE of trophozoites (Fig. 2F, lanes 1 and 2), whereas rabbit antibodies against rEhDEAD1$_{48}$ recognized a 48 kDa band in both CE and NE (Fig. 2F, lanes 3 and 4). As a control, we used antibodies against the *E. histolytica* Poly(A) polymerase (EhPAP) protein (Garcia-Vivas et al., 2005) that recognized the previously reported 63 kDa band in both CE and NE (Fig. 2F, lanes 5 and 6). In addition, anti-EhPC4 antibodies only detected the transcription and polyadenylation factor EhPC4 in the nucleus (Fig. 2F, lanes 7 and 8), demonstrating the absence of cross-contamination between both fractions. Our results suggested that the full-length 66.2 kDa EhDEAD1 was not present in trophozoites, but it was expressed as a smaller 48 kDa protein in both nuclear and cytoplasmic compartments.

Cellular location of EhDEAD1 was further confirmed by confocal microscopy of fixed trophozoites. Rabbit polyclonal antibodies anti-rEhDEAD1$_{48}$ revealed the presence of the EhDEAD1 protein in cytoplasm as small dots and in some cells, fluorescence also appeared dispersed in the nucleus (Fig. 3). It has been reported that other helicases are able to shuttle between nucleus and cytoplasm to carry out RNA processing functions in both cellular compartments (Askjaer et al., 1999; Sekiguchi et al., 2004). Further experiments are required to determine if EhDEAD1 could also have a function in both cellular compartments.

3.4. *rEhDEAD1$_{48}$ forms complexes with RNA and exhibits ATPase activity in vitro*

Binding to RNA substrates is required for RNA helicase functions. The predicted aa sequence of EhDEAD1 protein presents a putative RNA binding motif VI (Fig. 4A). To experimentally confirm that rEhDEAD1$_{48}$ binds to RNA, we carried out REMSA using the [α-^{32}P] UTP-labeled *EhPgp5* 3′UTR PSIII^{156} RNA probe. Results showed that the purified rEhDEAD1$_{48}$ interacted with the RNA probe in a concentration dependent manner (Fig. 4B and C). Densitometric analysis demonstrated that complex intensity was almost twice higher with 15 nM than with 5 nM of the purified enzyme (Fig. 4C). Radioactive complexes disappeared when unlabeled RNA probe was added to the reaction mixture, showing the specificity of the reaction. Additionally, RNA–protein complex formation was abolished by RNase or proteinase K treatments (Fig. 4B).

The energy used by RNA helicases to perform RNA binding and unwinding comes from ATP hydrolysis that is catalyzed by the ATPase domain formed by motifs I and II (also known as Walker motifs A and B) (Linder, 2006), which interact with Q motif to perform ATPase activity (Tanner et al., 2003). The full-length *EhDead1* gene has the 27 bp (450–477 nt position) that codify for the nine residues of Q motif (150–158 aa). As

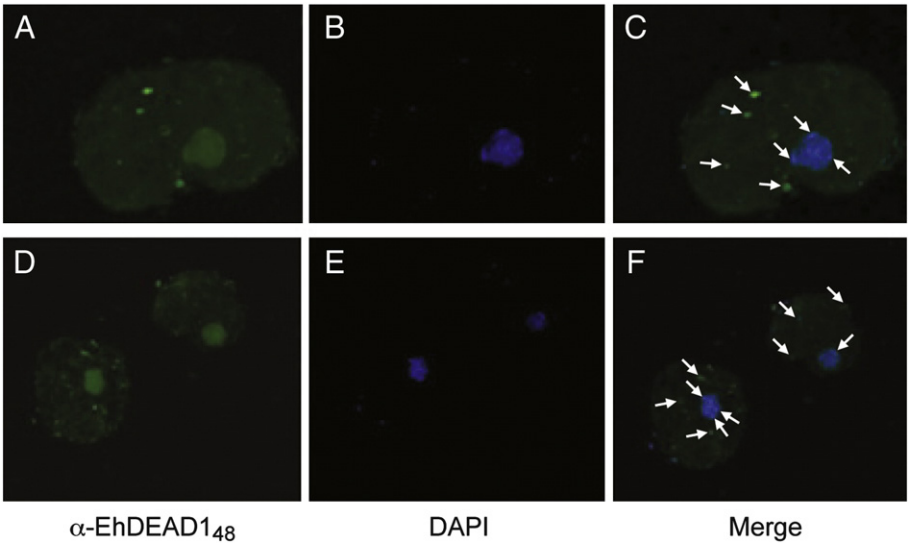

Fig. 3. Cellular localization of EhDEAD1. Trophozoites of clone A were incubated with rabbit anti-rEhDEAD1$_{48}$ antibodies, treated with FITC-labeled secondary antibodies, counterstained with DAPI and analyzed through confocal immunofluorescence microscopy. (A and D), cells observed in the green channel (FITC). (B and E), cells observed in the blue channel (DAPI). (C and F), cells simultaneously observed in both channels. Arrows, EhDEAD1 signal in cytoplasm and nucleus.

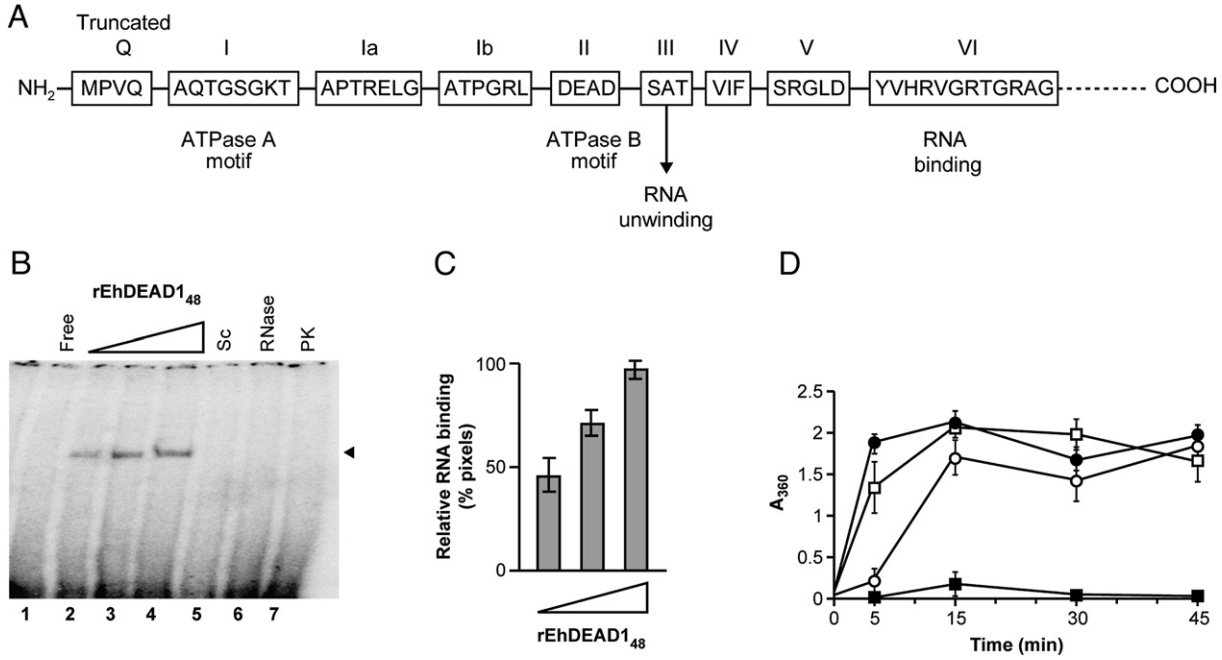

Fig. 4. RNA binding and ATPase activities of rEhDEAD1$_{48}$. (A) Schematic representation of rEhDEAD1$_{48}$ motifs. (B) REMSA. rEhDEAD1$_{48}$ was incubated with [α-^{32}P]UTP-labeled *EhPgp5* 3′UTR PSIII^{156} RNA probe (5×10^5 cpm) at 4 °C for 15 min. Complexes were resolved through 6% non-denaturing PAGE and detected in a Phosphor Imager apparatus. Lane 1, free probe; lane 2, RNA probe plus 5 nM rEhDEAD1$_{48}$; lane 3, RNA probe plus 10 nM rEhDEAD1$_{48}$; lane 4, RNA probe plus 15 nM rEhDEAD1$_{48}$; lane 5, as in lane 3 plus specific competitor (sc) (350-fold molar excess of unlabeled probe); lane 6, as in lane 3 plus RNase; lane 7, as in lane 3 plus proteinase K (PK). Arrowhead, RNA–protein complex. (C) Densitometric analysis of bands in B (lanes 2-4). Pixels in each band were obtained using the Quantity One software (Phosphor Imager apparatus). (D) ATPase activity of rEhDEAD1$_{48}$ was monitored as described in Section 2.8, in the presence of *E. histolytica* (□) or yeast (●) total RNA, *E. histolytica* poly(A$^+$) RNA (○) or without RNA (■).

described above, the rEhDEAD1$_{48}$ protein initiates at the third Met residue of the full-length predicted EhDEAD1 protein, lacking a 154 aa region that includes the first five residues of Q motif (Fig. 4A). We investigated if, even when it has a half truncated Q motif (155–158 aa), the rEhDEAD1$_{48}$ presented ATPase activity, using the EnzChek Phosphate Assay Kit (Molecular Probes) that monitors Pi release by the enzyme through its utilization in the MESG/PNP reaction. Five minutes after addition of 5 nM rEhDEAD1$_{48}$ in the reaction mixture containing *E. histolytica* total RNA (see Section 2.9), A_{360} value increased from 0 to 1.9 and this value was maintained through 45 min, indicating Pi release by rEhDEAD1$_{48}$ ATPase activity (Fig. 4D). rEhDEAD1$_{48}$ catalyzed ATP hydrolysis with the same efficiency in the presence of *S. cerevisiae* total RNA used as a control. When we used *E. histolytica* poly(A$^+$) RNA, A_{360} value increase appeared at 15 min incubation. No A_{360} increase was observed when we omitted RNA in the reaction (Fig. 4D). Results showed that rEhDEAD1$_{48}$ has ATPase activity even when it has a truncated Q motif. Activity was not spontaneous, but depends on the presence of RNA. The fact that Pi utilization appeared to be delayed when we used *E. histolytica* polyadenylated transcripts suggests that rEhDEAD1$_{48}$ has a higher ATPase activity in the presence of rRNA, tRNA or other RNA substrates contained in total RNA, than in the presence of poly(A$^+$) RNA. It is possible that specific secondary and tertiary RNA structures could modulate rEhDEAD1$_{48}$ ATPase activity, as it has been reported for other RNA helicases (Yang and Jankowsky, 2005).

3.5. rEhDEAD1$_{48}$ has ATP-dependent RNA unwinding activity in vitro

The fundamental function of DEAD-box RNA helicases is the RNA unwinding to allow transcription, ribosome biogenesis, pre-mRNA processing, mRNA export, degradation, interference, translation and other cellular activities involving RNA. The predicted aa sequence of EhDEAD1 contains the putative motif III involved in RNA unwinding (Linder, 2006) (Fig. 4A). To test the rEhDEAD1$_{48}$ RNA unwinding activity *in vitro*, we generated a partial heteroduplex RNA molecule with two 5′-overhangs using 216 and 246 nt ssRNA fragments (Fig. 5A). The rEhDEAD1$_{48}$ helicase activity was monitored through PAGE by the detection of ssRNA molecules that were separated from the heteroduplex RNA. In reactions containing 5 nM of rEhDEAD1$_{48}$ and 20 mM ATP, we detected three bands in the gel. The slowest migration band corresponds to the heteroduplex RNA (216–246 nt) and the fastest ones, to the 216 and 246 nt ssRNA molecules (Fig. 5B, lane 2). The presence of ssRNA bands in the gel evidenced the *in vitro* RNA unwinding activity of rEhDEAD1$_{48}$. Poor heteroduplex RNA dissociation was detected when ATP was omitted, showing that RNA unwinding was ATP-dependent (Fig. 5A, lanes 4 and 5). Additionally, the amount of heteroduplex RNA molecule remained almost unchanged when we used 10 nM purified rEhDEAD1$_{48}$ (Fig. 5B, lane 3), suggesting that EhDEAD1 could also have a strand annealing activity in these conditions. A similar capacity to promote both duplex unwinding and ssRNA molecules

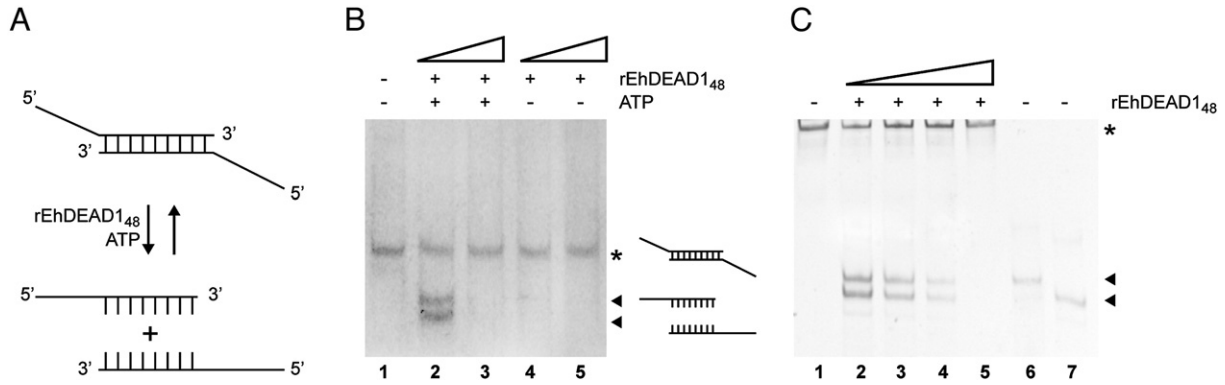

Fig. 5. RNA unwinding activity of rEhDEAD1$_{48}$. (A) Schematic representation of the heteroduplex RNA generation. (B) RNA unwinding assay. 500 ng of heteroduplex RNA was incubated with rEhDEAD1$_{48}$ in the presence (+) or absence (−) of ATP for 30 min at 37 °C. Samples were resolved through 12% non-denaturing PAGE and detected in a Phosphor Imager apparatus. Lane 1, free heteroduplex RNA; lanes 2–5, heteroduplex RNA incubated with 5 nM (lanes 2 and 4) and 10 nM (lanes 3 and 5) of rEhDEAD1$_{48}$, with (lanes 2 and 3) or without (lanes 4 and 5) ATP. Right, RNA molecules schemes. (C) RNA unwinding assay. 500 ng of heteroduplex RNA was incubated with rEhDEAD1$_{48}$ in the presence of ATP for 30 min at 37 °C. Lane 1, free heteroduplex RNA; lanes 2–5, heteroduplex RNA incubated with 2 nM (lane 2), 4 nM (lane 3), 8 nM (lane 4) and 16 nM (lane 5) of rEhDEAD1$_{48}$; lane 6, ssRNA molecule of 246 nt; lane 7, ssRNA molecule of 216 nt; Asterisk, dsRNA heteroduplex.

annealing *in vitro* has been previously reported for human p68 RNA helicase (Rossler et al., 2001) and yeast DED1 (Yang and Jankowsky, 2005). It is also possible that certain contaminants present in the partially purified rEhDEAD1$_{48}$ fraction could inhibit enzymatic activity. To confirm if the EhDEAD1 helicase function is affected by enzyme concentration, we evaluated RNA helicase activity across a range of 2 to 16 nM protein amounts. We observed RNA unwinding activity at 2, 4 and 8 nM (Fig. 5C, lanes 2–4), however activity was undetectable when we used 12 nM protein (Fig. 5C, lane 5), confirming results presented in Fig. 5B. Taken altogether, functional assays indicated that rEhDEAD1$_{48}$ exhibits RNA binding, ATPase and ATP-dependent RNA unwinding activities *in vitro*.

3.6. EhDead1 mRNA is over expressed in S phase of cell cycle

EhDEAD1 exhibits 70% homology to yeast DED1 RNA helicase (Table 1), which participates in cell cycle regulation (Warbrick and Glover, 1994; Forbes et al., 1998; Grallert et al., 2000). Although axenic cultures of *E. histolytica* are made of a heterogeneous population of cells with varying DNA content, various studies have described cell cycle phases in log phase cultures in distinct strains or clones (Orozco et al., 1988; Dvorak et al., 1995; Gangopadhyay et al., 1997; Vohra et al., 1998; Das and Lohia 2002; Dastidar et al, 2007). Here, we used trophozoites of clone L6, which is routinely synchronized by the mitotic blocker colchicine in our laboratory and whose cell cycle phases lasting is well characterized (Orozco et al., 1988; Marchat et al., 2003). As shown in Fig. 6A, [^{3}H] thymidine incorporation analysis confirmed that culture of L6 clone was synchronized by colchicine, exhibiting three cell cycles of about 12 h. At 20, 32 and 44 h, we observed a decrease in cpm number that corresponds to a doubling in cell number, indicating that synchronized trophozoites had passed through mitosis.

To investigate if the expression of the *EhDead1* gene varied throughout *E. histolytica* cell cycle phases, we first performed RT-PCR assays using RNA from synchronized trophozoites of clone L6. Using *EhDead1b-S* and *EhDead1b-AS* primers that

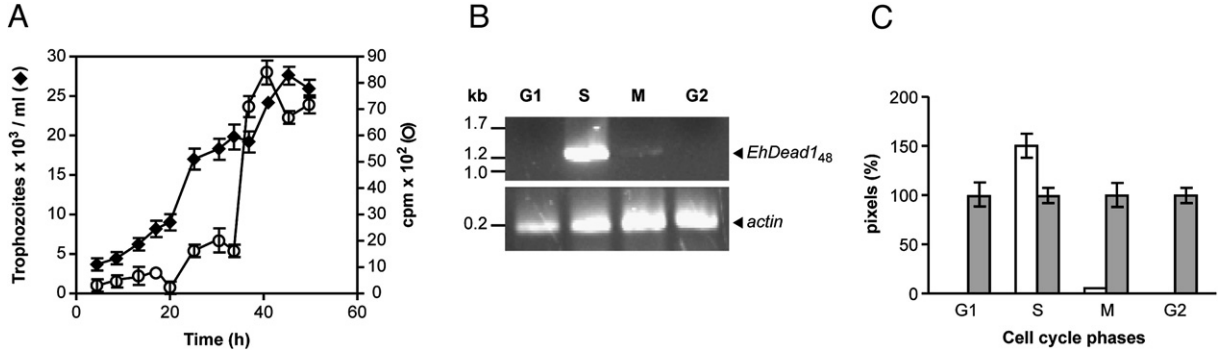

Fig. 6. Analysis of *EhDead1* mRNA expression through cell cycle. (A) Cell cycle synchronized culture of clone L6. Trophozoites were grown in TYI-s-33 medium with 200 mg/ml colchicines for 24 h before being transferred to fresh medium. Then, cell number and [^{3}H] incorporation were determined at 4 h intervals for 48 h. (B) RT-PCR assays. *EhDead1* and *actin* genes were simultaneously amplified using 1 μg of total RNA of cell cycle synchronized trophozoites (clone L6). Products were analyzed in 1% agarose gel. Arrowhead, amplified products. (C) Densitometric analysis of RT-PCR amplified products in B. Pixels corresponding to *actin* product were taken as 100% in each phase and used to normalize *EhDead1* products. White bars, *EhDead1$_{48}$* transcript; grey bars, *actin* transcript.

amplify from 465 to 1734 nt, we detected the 1.3 kb *EhDead1*$_{48}$ mRNA in S and M phases. Normalization with *actin* mRNA showed that *EhDead1*$_{48}$ mRNA was about 30-fold more abundant in S phase than in M phase (Fig. 6B and C), indicating that *EhDead1* gene transcription is regulated through cycle progression.

3.7. Antisense inhibition of EhDead1 mRNA expression seems to affect cell cycle progression

To further investigate the potential role of EhDEAD1 in cell cycle, we blocked *EhDead1* mRNA expression by transfecting trophozoites with the p*Neo-EhDead1-AS* plasmid containing the *EhDead1* antisense sequence (Fig. 7A). As a control, we transfected trophozoites with the p*Neo-CAT* plasmid lacking antisense *EhDead1-AS* DNA fragment. The presence of the plasmids in transfected trophozoites was confirmed by PCR amplification of the neomycin-resistance gene (Fig. 7B, lanes 2 and 3). As expected, RT-PCR assays evidenced the *EhDead1*$_{48}$ transcript in trophozoites transfected with the p*Neo-CAT* plasmid and non-transfected trophozoites. In contrast, no *EhDead1*$_{48}$ mRNA was found in trophozoites transfected with p*Neo-EhDead1-AS*, indicating that the *EhDead1* transcript was blocked by the antisense construction (Fig. 7C). As a control, endogenous *actin* DNA and mRNA was amplified in wild-type and transfected trophozoites (Fig. 7B and C). Growth and morphology of transfected and not transfected trophozoites were not significantly different (data not shown).

Next, DNA synthesis was inhibited by serum starvation in transfected and non-transfected trophozoites (Vohra et al., 1998) and then, cell cycle reactivation was induced by addition of fresh medium and DNA content was analyzed by flow cytometry (Fig. 7D and E). In non-transfected cultures, 62.1±7.5% of trophozoites were in G0/G1 phases, 36.5±5.9% in S phase and only 0.6±0.5% in G2/M phases (Fig. 7D). Similar values were obtained using trophozoites transfected with the p*Neo-CAT* plasmid (data not shown). These results confirm that most trophozoites were arrested in G0/G1 phase due to serum starvation and that cell cycle was progressively reactivated when cells were changed to fresh complete medium. In trophozoites transfected with p*Neo-EhDead1-AS* plasmid, 63.9±5.6% of the cells were in G0/G1 phase, 23.5±2.2% in S phase, and 12.4±3.8% appeared in G2/M phase (Fig. 7E). Analysis of experimental data by the *t* test showed that the percentage of cells in S

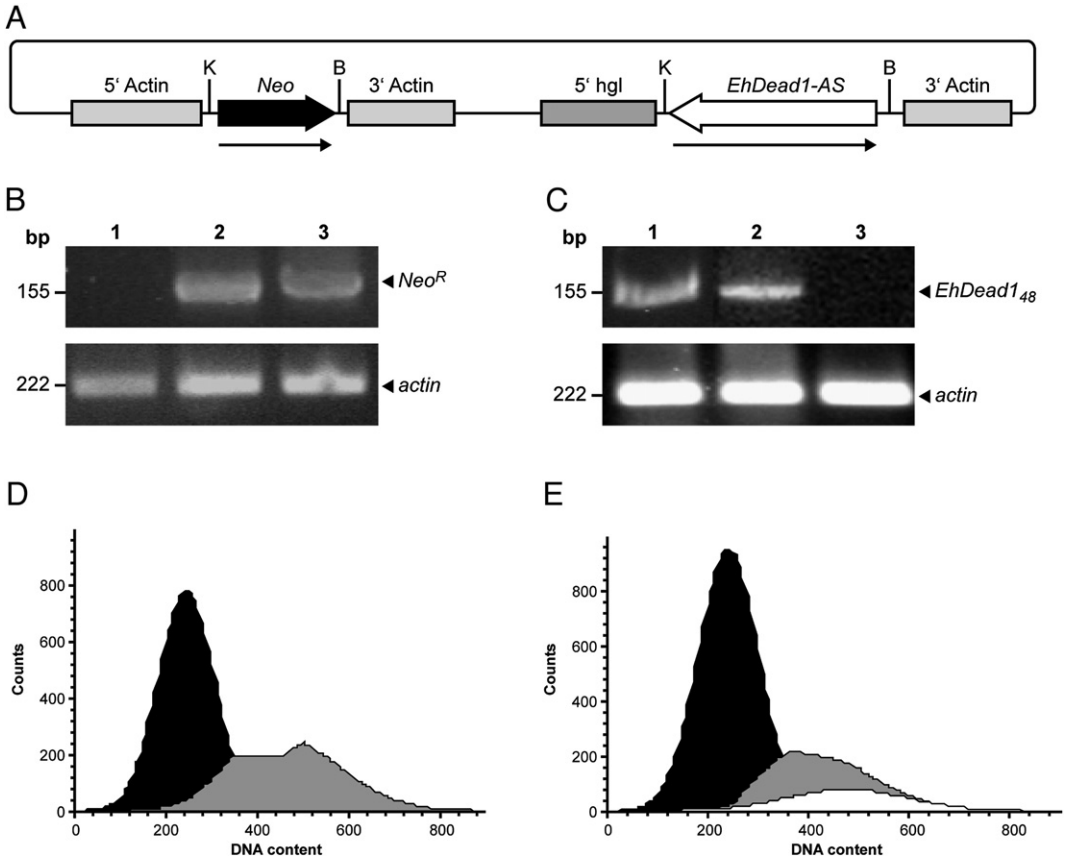

Fig. 7. Inhibition of *EhDead1* gene expression using antisense RNA and its effects on cell cycle progression. (A) Schematic depiction of *pNeo-EhDead1*-AS plasmid. The antisense cassette was constructed by inserting the *EhDead1* gene into the KpnI (K) and BamHI (B) restriction sites of *pNeo-CAT*. Thin arrow, transcription orientation; Open arrow, gene orientation. (B) PCR amplification of neomycin-resistance (*neo*^{r}) and *actin* genes. Lane 1, wild-type trophozoites; lane 2, *pNeo-CAT* transfected trophozoites; lane 3, *pNeo-EhDead1*-AS transfected trophozoites. (C) RT-PCR amplification of *EhDead1* and *actin* transcripts. Lane 1, wild-type trophozoites; lane 2, *pNeo-CAT* transfected trophozoites; lane 3, *pNeo-EhDead1*-AS transfected trophozoites. (D–E) Representative flow cytometry analysis of wild-type (D) and *pNeo-EhDead1*-AS transfected (E) trophozoites arrested by serum deprivation. Graphics show the DNA content in the *X*-axis and cells number in *Y*-axis. Black curve, G0/G1 phase; grey curve, S phase; white curve, G2/M phase.

and G2/M phase was significantly different in non-transfected and transfected cultures ($p<0.05$), whereas no differences were observed for cells in G0/G1 phase ($p=0.74$). Our results indicated that *EhDead1* mRNA inhibition was associated with a slight reduction of trophozoites in S phase and an increased number of cells in G2/M phase.

3.8. EhDEAD1 did not rescue the temperature sensitive ded1p yeast mutants

YTC180 and YTC181 yeast strains contain the *ded1-120* and *ded1-119* mutant alleles of the *Ded1* gene, respectively. Both mutant strains grow as well as the wild-type strain (YTC74) at permissive conditions (30 °C), but they do not grow at restrictive temperature (15 °C), due to severe deficiencies in protein synthesis (Chuang et al., 1997). Since EhDEAD1 exhibits high homology with yeast DED1 RNA helicase, we investigated if *EhDead1* gene could complement the conditional yeast *Ded1* mutant strains. YTC180 and YTC181 were transformed with either pDED1008 or pRS316-*EhDead1,* and grown at permissive conditions in the corresponding selective media. As expected, YTC74 strain grew at 30 °C and 15 °C, while YTC180 and YTC181 strains only grew at permissive temperature (30 °C) (Supplementary data Fig. S1A). Mutant strains transformed with yeast pDED1008 (JP3 and JP4) grew at 15 °C and 30 °C, whereas those transformed with pRS316-*EhDead1* (JP1 and JP2) only grew at 30 °C (Supplementary data Fig. S1A), showing that *E. histolytica Ehdead1* gene was not able to complement yeast mutant genes. To discard that the absence of functional complementation was due to lack of *EhDead1* gene expression in transformed yeast, we performed RT-PCR assays with $EhDead1_{48}$ specific primers. Results showed the presence of the $EhDead1_{48}$ transcript in pRS316-*EhDead1* transfected yeast (Supplementary data Fig. S1B), demonstrating that *EhDead1* gene was transcribed although EhDEAD1 was unable to rescue mutant yeast.

4. Discussion

Analysis of the recently completed *E. histolytica* genome sequence showed the existence of a large DEAD–DExH-box RNA helicases family (Marchat et al., submitted for publication), suggesting that these proteins have active roles in the fine tuning of transcription, mRNA processing and degradation, as well as translation in this parasite, probably remodeling RNA secondary structures to dissociate RNA–RNA or RNA–protein complexes. Here, we present the cloning, expression and functional characterization of a novel RNA helicase in *E. histolytica*, EhDEAD1. Bioinformatics analysis of the predicted aa sequence of EhDEAD1, including the central core region with the nine consensus motifs of the helicase domain, indicated that EhDEAD1 is a well conserved orthologue of DEAD-box RNA helicases described in various organisms through evolutionary scale, confirming the initial TIGR and Pathema annotation.

Northern blot and RT-PCR assays showed that the *EhDead1* gene reported in the locus EHI-175030 of the *E. histolytica* genome database is not fully transcribed. As a result, Western blot assays evidenced the presence of a protein smaller than expected in trophozoites. Based on our results, we propose that the *EhDead1* gene reported at locus EHI-175030 is not transcribed from the first ATG codon, but from the third one located at 462 nt. It is also possible that the full-length *EhDead1* transcript is postranscriptionally processed to generate a shorter mRNA of 1.3 kb that is translated to a 48 kDa protein with a half truncated Q motif. Another possibility is that the gene prediction in Pathema database may be incorrect for the clone A trophozoites used here. The presence of EhDEAD1 in nucleus and cytoplasm of trophozoites is not surprising because RNA unwinding could be occurring in both cellular compartments during nuclear pre-mRNA processing and cytoplasmic mRNA stabilization, translation and degradation. In fact, other DEAD-box RNA helicases have been found shuttling between nucleus and cytoplasm to perform their functions (Askjaer et al., 1999; Yedavalli et al., 2004; Sekiguchi et al., 2004).

The $rEhDEAD1_{48}$ protein expressed in *E. coli* was purified to initiate its functional characterization. $rEhDEAD1_{48}$ has RNA-dependent ATPase activity *in vitro*, even when it has an incomplete Q motif, suggesting that the first aa of the Q motif are not essential for $rEhDEAD1_{48}$ ATPase *in vitro* activity. However, we cannot discard that the presence of the complete Q motif could enhance ATPase activity *in vitro* and *in vivo*. Assays using *E. histolytica* and yeast total RNA indicated that $rEhDEAD1_{48}$ ATPase activity is not restricted to parasite RNA substrates. The fact that ATPase activity was lower in the presence of *E. histolytica* poly(A)$^+$ RNA suggest that that EhDEAD1 function could be more related to other RNA molecules, such as tRNA or rRNA, at least *in vitro*. These observations may not reflect the *in vivo* situation, where additional proteins could provide RNA specificity to *E. histolytica* enzyme. For example it has been demonstrated that yeast DED1 function can be controlled by an RNA binding protein that does not directly interact with DED1 (Bowers et al., 2006).

In a standard assay, $rEhDEAD1_{48}$ was able to unwind heteroduplex RNA molecules with 5′ overhangs, demonstrating the basic biochemical function of the enzyme. In our experimental conditions, $rEhDEAD1_{48}$ also exhibited a potential ssRNA reannealing activity at higher concentrations. A similar capacity to promote both duplex unwinding and strand annealing *in vitro* had been previously reported for several DEAD-box proteins from human (Rossler et al., 2001) and yeast (Yang and Jankowsky, 2005). In addition to the conserved helicase domain, the carboxyl terminus of these proteins, including EhDEAD1, presents the characteristic clusters of arginine and glycine residues that have been shown to contribute to the annealing activity of yeast DED1 (Yang and Jankowsky, 2005). Further experiments using unlabeled oligonucleotides, other RNA substrates (3′ overhangs or blunt-ends templates) and different ATP concentrations will allow a better characterization of both RNA unwinding and strand annealing activities of rEhDEAD1 protein.

Experimental assays to investigate the biological relevance of EhDEAD1 in *E. histolytica* trophozoites indicated that it could be related to cell growth regulatory functions. Although G1, S, G2 and M phases have been described in *E. histolytica*, this

protozoan presents unusual cell cycle characteristics. Unlike most eukaryotes, *Entamoeba* trophozoites duplicate their genome several times before nuclear and cell divisions occur, generating multinucleated and polyploid cells (Gangopadhyay et al., 1997; Das and Lohia, 2002). It has been suggested that surveillance mechanisms or checkpoints regulating alternation of genome duplication and cell division are altered or absent in *E. histolytica*. Sequence homologous to several cell cycle regulating proteins have been identified in amoeba, but their structural divergence suggests that they may not have equivalent function in this organism (Banerjee et al., 2002; Lohia, 2003;Loftus et al., 2005; Lohia et al., 2007). Constitutive association of the evolutionary conserved EhMcm2-3-5 proteins with chromatin could be one of the reasons why genome reduplication occurs in *E. histolytica* (Das et al., 2005). EhKlp5, a divergent member of the kinesin 5 family, is essential for microtubular assembly, genome content and cell division in *E. histolytica* (Dastidar et al., 2007).

The finding that *EhDead1* gene was mainly transcribed in cell cycle S phase suggested that the EhDEAD1 RNA helicase might be involved in S phase and/or posterior cell cycle steps (G2, M) or boundaries. Moreover, it was consistent with the observation that S to G2/M transition seemed to be facilitated when *EhDead1* gene expression was inhibited by antisense RNA. Although they did not allow determining a precise role for EhDEAD1 in *E. histolytica*, our results suggested that this protein could be involved in some checkpoints during or after the S phase, probably remodeling RNA structures or RNA–protein complexes that are important for cell cycle progression. In the absence of EhDEAD1, these checkpoints could be inactive, allowing cells to pass faster from S phase to G2/M phases. However, additional experiments are required to establish the precise role of EhDEAD1 in cell cycle progression. The participation of DEAD-box helicases in growth and cell cycle control has been previously described in other organisms. In mouse, genetic knockdown of DDX3 in NIH-3T3 cells line results in an enhancement of cell cycle progression that is linked to the upregulation of cyclin D1 and the downregulation of $p21^{WAF1}$ (Chang et al., 2006). In human, the phosphorylation of the p68 RNA helicase promotes cell proliferation by activating the transcription of cyclin D1 and other genes (Yang et al., 2007).

The fact that yeast *dead1-120* and *dead1-199* cold-sensitive mutants were not functionally replaced by *E. histolytica* EhDEAD1 protein, suggested that EhDEAD1 and yeast DED1 are not functionally conserved in spite of their high sequence similarity. Notably, Gly residues at position 108, 368 and 494, which are replaced by Asp in yeast mutants (Chuang et al., 1997), are present in conserved positions in the EhDEAD1 protein. The possible participation of EhDEAD1 in biological processes that are different from those involving eukaryotic orthologous proteins, adds even more complexity to the understanding of these enzymes. It is also possible that yeast DED1 activation requires the interaction with specific factors that are unable to interact with EhDEAD1 to rescue the temperature sensitive mutants. Additionally, the amino terminus that differs in both proteins could have an effect in complementation experiments.

In summary, our results showed that recombinant EhDEAD1 exhibits RNA binding, ATPase, and ATP-dependent RNA unwinding activities *in vitro* and seems to have a role in cell cycle. Experimental work currently in progress will help us to define the specific RNA substrates and the biological function of EhDEAD1 in *E. histolytica* trophozoites.

Acknowledgements

The *EhDead1* gene sequence was obtained from TIGR and Sanger *E. histolytica* genome sequence databases. We thank Dr. Jean-Leon Chong from the Department of Molecular Genetics at the Ohio State University for generously providing the yeast *Ded1* mutants. We are grateful to M. en C. Victor Rosales from the Central Laboratory of CINVESTAV-IPN for helping us with the acquisition of the data on CompuCyte. Our thanks are also to Alfredo Padilla and Sollange Archer for their help in the artwork. This work was supported by UACM (Mexico), CONACyT (Mexico), COFAA-IPN (Mexico) and SIP-IPN (Mexico) grants.

Appendix A. Supplementary data

Supplementary data associated with this article can be found, in the online version, at doi:10.1016/j.gene.2008.01.024.

References

Askjaer, P., et al., 1999. RanGTP-regulated interactions of CRM1 with nucleoporins and a shuttling DEAD-box helicase. Mol. Cell. Biol. 19, 6276–6285.

Banerjee, S., Das, S., Lohia, A., 2002. Eukaryotic checkpoints are absent in the cell division cycle of *Entamoeba histolytica*. J. Biosciences 27, 567–572.

Bowers, H., et al., 2006. Discriminatory RNP remodeling by the DEAD-box protein DED1. RNA 2, 903–912.

Chang, P.C., et al., 2006. DDX3, a DEAD box RNA helicase, is deregulated in hepatitis virus-associated hepatocellular carcinoma and is involved in cell growth control. Oncogene 25, 1991–2003.

Chuang, R., Weaver, P., Liu, Z., Chang, T., 1997. Requirement of the DEAD-box protein Ded1p for messenger RNA translation. Science 275, 1468–1471.

Das, S., Lohia, A., 2002. Delinking of S phase and cytokinesis in the protozoan parasite *Entamoeba histolytica*. Cell. Microbiol. 4, 55–60.

Das, S., Mukherjee, C., Sinha, P., Lohia, A., 2005. Constitutive association of Mcm2-3-5 proteins with chromatin in *Entamoeba histolytica*. Cell. Microbiol. 7, 259–267.

Dastidar, P.G., Majumder, S., Lohia, A., 2007. Eh Klp5 is a divergent member of the kinesin 5 family that regulates genome content and microtubular assembly in *Entamoeba histolytica*. Cell. Microbiol. 9, 316–328.

Diamond, L.S., Harlow, R., Cunnick, C., 1978. A new medium for the axenic cultivation of *Entamoeba histolytica* and other *Entamoeba*. Trans. R. Soc. Trop. Med. Hyg. 72, 431–432.

Dillon, P.J., Rosen, C.A., 1990. A rapid method for the construction of synthetic genes using the polymerase chain reaction. BioTechniques 9, 298–300.

de Dios-Bravo, G., Luna-Arias, J.P., Riveron, A.M., Olivares-Trejo, J.J., Lopez-Camarillo, C., Orozco, E., 2005. *Entamoeba histolytica* TATA-box binding protein binds to different TATA variants in vitro. FEBS J. 272, 1354–1366.

Dvorak, J.A., Kobayashi, S., Alling, D.W., Hallahan, C.W., 1995. Elucidation of the DNA synthetic cycle of *Entamoeba* spp. using flow cytometry and mathematical modeling. J. Eukaryotic Microbiol 42, 610–616.

Forbes, K.Ch., Humphrey, T., Enoch, T., 1998. Suppressors of Cdc25p overexpression identify two pathways that influence the G2/M checkpoint in fission yeast. Genetics 150, 1361–1375.

Fuller-Pace, F.V., 2006. DExD/H box RNA helicases: multifunctional proteins with important roles in transcriptional regulation. Nucleic Acids Res. 34, 4206–4215.

Gangopadhyay, S.S., Ray, S.S., Kennady, K., Pande, G., Lohia, A., 1997. Heterogeneity of DNA content and expression of cell cyclegenes in

axenically growing *Entamoeba histolytica* HM1:IMSS clone A. Mol. Biochem. Parasitol. 90, 9–20.

Garcia-Vivas, J., Lopez-Camarillo, C., Azuara-Liceaga, E., Orozco, E., Marchat, L.A., 2005. *Entamoeba histolytica*: cloning and expression of the poly(A) polymerase EhPAP. Exp. Parasitol. 110, 226–232.

Gorbalenya, A., Koonin, E., 1993. Helicases: amino acid sequence comparisons and structure–function relationships. Curr. Opin. Struct. Biol. 3, 419–429.

Grallert, B., et al., 2000. A fission yeast general translation factor reveals links between protein synthesis and cell cycle controls. J. Cell. Sci. 113, 1447–1458.

Gururajan, R., Prryokeefe, H., Melton, D.A., Weeks, D.L., 1991. The *Xenopus* localized messenger RNA An3 may encode an ATP-dependent RNA helicase. Nature 349, 717–719.

Hamann, L., Nickel, R., Tannich, E., 1995. Transfection and continuous expression of heterologous genes in the protozoan parasite *Entamoeba histolytica.* Proc. Natl. Acad. Sci. USA 92, 8975–8979.

Ivens, A.C., et al., 2005. The genome of the kinetoplastid parasite, *Leishmania major.* Science 309, 436–442.

Jackson, T.F., 2000. Epidemiology. In: Ravdin, J.I. (Ed.), Amebiasis. Imperial College Press, London, pp. 47–63.

Kumar, S., Tamura, K., Nei, M., 2004. MEGA3: integrated software for molecular evolutionary genetics analysis and sequence alignment. Brief. Bioinform. 5 (2), 150–163.

Linder, P., 2006. Dead-box proteins: a family affair-active and passive players in RNP-remodeling. Nucleic Acids Res. 34, 4168–4180.

Linder, P., Daugeron, M., 2000. Are DEAD-box proteins becoming respectable helicases? Nat. Struct. Biol. 7, 97–99.

Lohia, A., 2003. The cell cycle of *Entamoeba histolytica*. Mol. Cell. Biochem. 253, 217–222.

Lohia, A., Mukherjee, C., Majumder, S., Dastidar, P.G., 2007. Genome re-duplication and irregular segregation occur during the cell cycle of *Entamoeba histolytica*. Biosci. Rep. 26 [Electronic publication ahead of print].

Loftus, B., et al., 2005. The genome of the protist parasite *Entamoeba histolytica*. Nature 433, 865–868.

Lopez-Camarillo, C., Luna-Arias, J.P., Marchat, L.A., Orozco, E., 2003. *EhPgp5* mRNA stability is a regulatory event in the *Entamoeba histolytica* multidrug resistance phenotype. J. Biol. Chem. 278, 11273–11280.

Lopez-Camarillo, C., Orozco, E., Marchat, L.A., 2005. *Entamoeba histolytica*: comparative genomics of the pre-mRNA 3¢ end processing machinery. Exp. Parasitol. 110, 184–190.

Marchat, L.A., Gomez, C., Perez, D., Paz, F., Mendoza, L., Orozco, E., 2002. Two CCAAT/enhancer binding protein sites are *cis*-activator elements of the *Entamoeba histolytica EhPgp1* (*mdr*-like) gene expression. Cell. Microbiol. 4, 725–737.

Marchat, L.A., Pezet-Valdez, M., López-Camarillo, C., Orozco, E., 2003. *Entamoeba histolytica*: expression and DNA binding of CCAAT/enhancer binding proteins are regulated through the cell cycle. Exp. Parasitol. 103, 82–87.

Mendoza, L., et al., 2003. Ehp53, an *Entamoeba histolytica* protein, ancestor of the mammalian tumour suppressor p53. Microbiology 149, 885–893.

Orozco, E., Solis, F., Dominguez, J., Chavez, B., Hernandez, F., 1988. *Entamoeba histolytica*: cell cycle and nuclear division. Exp. Parasitol. 67, 85–95.

Rocak, S., Linder, P., 2004. DEAD-BOX proteins: the driving forces behind RNA metabolism. Nat. Rev. Cell. Biol. 5, 232–241.

Rossler, O., Straka, A., Stahl, H., 2001. Rearrangement of structured RNA via branch migration structures catalysed by the highly related DEAD-box proteins p68 and p72. Nucleic Acids Res. 29, 2088–2096.

Schwer, B., 2001. A new twist on RNA helicases: DExH/D box proteins as RNPases. Nat. Struct. Biol. 8, 113–116.

Sekiguchi, T., Lida, H., Fukumura, J., Nishimoto, T., 2004. Human DDX3Y, the Y-encoded isoform of RNA helicase DDX3, rescues a hamster temperature-sensitive ET24 mutant cell line with a DDX3X mutation. Exp. Cell. Res. 300, 213–222.

Tanner, N., Linder, P., 2001. DExD/H box RNA helicases: from generic motors to specific dissociation functions. Mol. Cell 8, 251–262.

Tanner, N.K., Cordin, O., Banroques, J., Doere, M., Linder, P., 2003. The Q motif: a newly identified motif in DEAD box helicases may regulate ATP binding and hydrolysis. Mol. Cell, 11, 127–138.

Tuteja, R., Pradhan, A., 2006. Unraveling the "DEAD-box" helicases of *Plasmodium falciparum*. Gene 376, 1–12.

Vohra, H., Mahaan, R.C., Ganguly, N.K., 1998. Role of serum deprivation in regulating the *Entamoeba histolytica* cell cycle: a flow cytometric analysis. Parasitol. Res. 84, 835–838.

Warbrick, E., Glover, D., 1994. A *Drosophila* gene encoding a DEAD box RNA helicase can suppress the loss of *wee1*/*mik1* function in *Schizosaccharomyces pombe*. Mol. Gen. Genet. 245, 654–657.

Webb, M., 1992. A continuous spectrophotometric assay for inorganic phosphate and for measuring phosphate release kinetics in biological systems. Proc. Natl. Acad. Sci. USA 89, 4884–4887.

Yang, Q., Jankowsky, E., 2005. ATP- and ADP-dependent modulation of RNA unwinding and strand annealing activities by the DEAD-box protein DED1. Biochemistry 44, 13591–13601.

Yang, L., Lin, C., Zhao, S., Wang, H., Liu, Z.R., 2007. Phosphorylation of p68 RNA helicase plays a role in platelet-derived growth factor-induced cell proliferation by up-regulating cyclin D1 and c-Myc expression. Biol. Chem. 282, 16811–16819.

Yedavalli, V., Neuveut, C., Chi, Y., Kleiman, L., Jeang, K., 2004. Requirement of DDX3 DEAD box RNA helicase for HIV-1 Rev-RRE export function. Cell 119, 381–392.